Density Functional Investigations of Defect-Induced Mid-Gap States in Graphane

Bhalchandra S. Pujari*,† and D. G. Kanhere†,‡

Department of Physics and Centre for Modelling and Simulations, University of Pune, Ganeshkhind, Pune-411 007, India

Received: August 7, 2009; Revised Manuscript Received: November 5, 2009

We have carried out ab initio electronic structure calculations on *graphane* (hydrogenated graphene) having single and double vacancy defects. Our analysis of the density of states reveals that such vacancies induce the mid-gap states and modify the band gap. The induced states are due to the unpaired electrons on carbon atoms surrounding the vacancy. Interestingly, the placement and the number of such states is found to be sensitive to the distance between the vacancies. It turns out that such vacancies also induce a local magnetic moment.

1. Introduction

Graphane, i.e., the hydrogenated graphene, is a recent addition to the family of novel carbon materials known for their exotic properties (to avoid confusion with the word "graphene", the word "*graphane*" is written in italics throughout this paper).[1−3] Recently *graphane* was experimentally realized by Elias et al.,[4] who demonstrated that the process of hydrogenation is reversible. This observation makes *graphane* a suitable candidate for hydrogen-storage materials. Equally interesting is the possibility of direct observation of metal−insulator transition in two-dimensional systems,[5] as a function of hydrogen coverage. *Graphane* is an insulator and the reported theoretical band gap with use of density functional theory (DFT) is ∼3.5 eV.[1]

It is well-known that a single sheet of graphene is susceptible to a variety of disorders like topological defects, impurity states, ripples, cracks, etc. Pereira et al.[6,7] have studied different models of local disorders in graphene and have investigated their electronic structure within the tight binding method. They have observed significant changes in the low-energy spectrum of graphene, viz., localized zero modes, strong resonances, the existence of gap and pseudogap, etc., depending upon the type of disorder. Their results also indicate that by and large disorder modifies the states near the Fermi level. Yazyev and Helm[8] have studied defect-induced magnetism in graphene within the DFT framework. Their work shows that the adsorption of hydrogen or the creation of defect on graphene sheet leads to the local magnetic moment. For an extensive survey of the studies and the disorder in graphene, we refer the reader to a recent review by Castro Neto et al.[9] We wish to point out that most of the novel properties of graphene arise due to the nature of the density of states (DOS) near the Fermi level and these states are sensitive to the presence of defects.

Quite clearly a detailed study of defect-induced states is warranted not only for graphene but also for *graphane*. So far there are no reports of systematic investigations of the effects of such defects on the properties of *graphane*. In the present work we focus on the electronic structure of *graphane* with topological defects created by removal of one and two carbon atoms. Such defects are experimentally realized by using high-energy ion beams as demonstrated by Jin et al.[10] by creating a stable carbon chain from a graphene sheet.

The present work is based on spin density functional theory (SDFT), which is known to underestimate the band gap. A recent calculation by Lebègue et al.[11] based on GW approximation estimated the band gap of *graphane* to be 5.4 eV. In the same work the authors have also shown that the removal of a single hydrogen atom produces mid-gap states.

The paper is organized as follows. We present the relevant computational details in section 2. In subsection 3.1, the results for pristine *graphane* are summarized for the sake of completion. The main results of the electronic structure calculations on the single and the double vacancy defects are presented in subsections 3.2 and 3.3, respectively. Finally the conclusions are presented in section 4.

2. Computational Details

All the calculations have been performed on a monolayer *graphane*, having geometry as described by Sofo et al.[1] We have used plane wave based DFT as implemented in Quantum Espresso (http://www.quantum-espresso.org/) for all the calculations. The single vacancy work has also been repeated with use of VASP.[12] It was found that the geometries, energies, and the DOS obtained from both codes are in good agreement despite using different pseudopotentials. All the results presented in the paper are obtained with Quantum Espresso. The generalized gradient approximation as given by Perdew, Burke, and Ernzerhof[13,14] has been used for the exchange-correlation potential. The electron smearing is kept at 0.05 eV. For a single vacancy study the primitive *graphane* cell is repeated 5 times in *X* and *Y* directions while for that of double vacancies the repetitions are of 7 units. A single vacancy means removing a single carbon atom along with the attached hydrogen. After removing two (four) atoms to form single (double) defect(s) there are a total of 98 (192) atoms on the *graphane* plane. The vertical axis (*Z*) of the cell is kept as large as 10 Å to avoid the interactions between the *graphane* sheets. The energy and force thresholds are kept at 10^{-6} eV and 10^{-5} eV/Å, respectively. It may be mentioned that even though the unit cell is large it was found to be necessary to use 5×5 Monkhorst-Pack *k*-grid for acceptable convergence in energy during the optimization and the self-consistency. After optimization we have used 11×11 Monkhorst-Pack *k*-grid for the final calculations of DOS and other quantities.

* To whom correspondence should be addressed.
† Department of Physics.
‡ Centre for Modelling and Simulations.

10.1021/jp907640t
Published on Web 11/23/2009

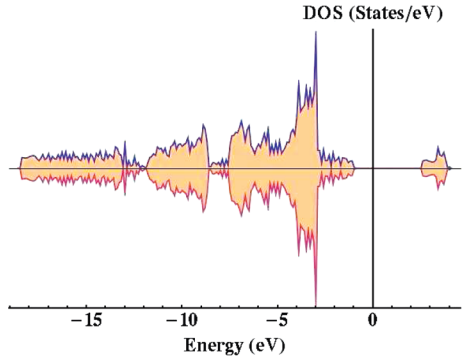

Figure 1. Spin-polarized total DOS for pristine *graphane*. The upper and lower halves of the graph represent up and down spins, respectively. The zero of the energy is taken as the Fermi energy and marked by a solid vertical line. The system is nonmagnetic with a band gap of ∼3.5 eV.

3. Results and Discussion

3.1. Pristine *Graphane*. Before we present the results of the vacancy studies, it is instructive to summarize the properties of a pure *graphane*. Our results on pristine *graphane* are consistent with the earlier reports.[1,2] *Graphane* is known to have two distinct conformations depending upon the position of hydrogen atoms with respect to the graphene plane. In the *chair* conformer the hydrogen atoms are attached to carbon atoms in alternating manner on both sides of the plane while in the *boat* conformer the pairs of hydrogen atoms are attached in alternating manner.[1] Out of these two the chair conformer is energetically more favorable, hence in the present work we have used the chair conformer only. It is interesting to note that in the case of graphene only a single *k*-point (Dirac point) of Brillouin zone is degenerate (no gap in DOS); however, in *graphane* the minimum gap is observed at the Γ point (∼3.5 eV) while the Dirac point develops a rather large gap at ∼12 eV.

We now discuss the DOS of pristine *graphane*, which is shown in Figure 1. The zero of the energy is taken as the Fermi energy and marked by a vertical line. The largest peak seen (at ∼ −3 eV) is due to the peculiar sp^3-like bonding between carbon and hydrogen. The states at the top of the valence band (∼ −1 eV) are mainly of p states forming σ bonds among the carbon atoms. Unlike graphene there are no π bonds in *graphane*.

3.2. Single Vacancy. We begin our discussion by presenting the results of a single vacancy with the focus on its effects on the geometry and electronic structure. Let us recall that a single vacancy means the absence of a single carbon atom along with attached hydrogen. The fully relaxed structure of such a vacancy is shown in Figure 2. The effect of the removal of the atoms is seen on the sublattice surrounding the vacancy (indicated by the triangle in the figure). In an ideal *graphane* the carbon sublattice is an equilateral triangle with the length of a side a = 2.52 Å. However, in the presence of a vacancy the sublattice deforms substantially. Due to reduced coordination number, three carbon atoms on the triangle are pushed away from each other and remain as a part of the hexagon. It may be noted that the distortion of the triangle is asymmetric, which is attributed to the Jahn−Teller effect. We wish to stress that the deformation seen here is qualitatively different than that seen in the case of graphene. In the later case two of the carbon atoms move close to each other to form a σ bond[8] giving rise to a five-ringed structure. On the contrary we do not see bond formation among the carbon atoms. Thus, the vacancy leaves three dangling bonds on the triangle. Two of the electrons screen the moment of each other and as a consequence, the system becomes magnetic with

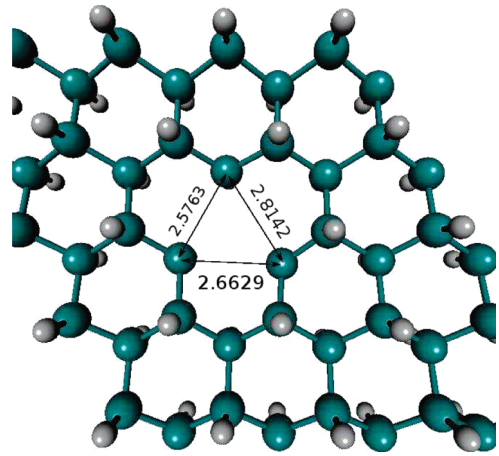

Figure 2. The optimized structure of *graphane* with a single vacancy. Carbon atoms are shown in cyan while hydrogen atoms are in white. The Jahn−Teller distortion of the sublattice surrounding the vacancy is clearly evident (marked by the triangle). The pristine sublattice is an equilateral triangle with a = 2.52 Å.

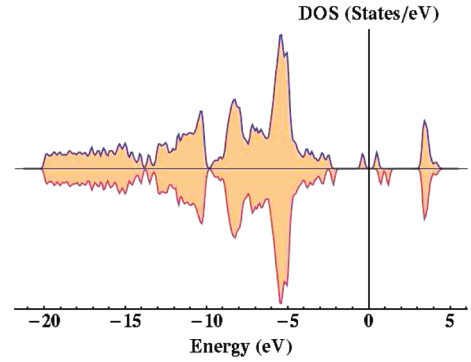

Figure 3. DOS of *graphane* with single vacancy displaying the induced states in the gap. Fermi energy is at zero and shown by the vertical line. The induced states are partially occupied for up electrons.

magnetic moment 1 μ_B. We have performed additional calculations with constrained magnetic moments and it turns out that the state with 1 μ_B is lower in energy with respect all other states by at least 0.05 eV. Apart from inducing magnetic moment the unpaired electrons also have some interesting effects on the DOS.

Figure 3 shows the spin polarized DOS displaying some remarkable features. The DOS with single vacancy is substantially different from that of pristine *graphane*[1] especially near the Fermi energy (marked by a vertical line in the figure). Clearly the vacancy has induced the *mid-gap* states which are partially occupied. In particular the induced spin-up states are partially occupied while the induced spin-down states are completely empty. The appearance of mid-gap states can be attributed to the unpaired electrons from the three nearest carbon atoms, due to which the states are pushed up from the valence band. To ascertain this observation we have hydrogenated three available dangling bonds. Our results show that increasing hydrogen concentration (from one to three) steadily reduces the density of induced states (figure not shown). Finally with complete hydrogenation, induced states vanish and the band gap reduces to ∼3 eV.

That the induced states are due to the unpaired electrons can also be seen from the examination of the site projected DOS. Figure 4 shows site projected DOS (PDOS) on one of the carbon atoms of the triangle. It can be seen that almost all the contribution to the mid-gap states comes from the three-carbon

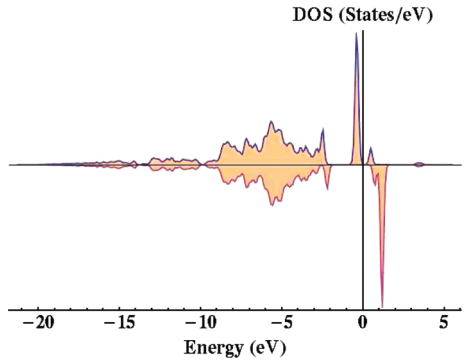

Figure 4. The site projected density of states (PDOS) on one of the carbon atoms surrounding the vacancy. It is evident that most of the contribution to the induced states come from the carbon atoms on the sublattice.

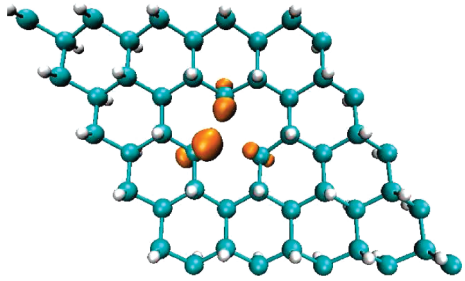

Figure 5. Isosurface of the charge density of the occupied state just below the Fermi level for the case of single vacancy. The state is dominantly p_x-p_y-like and is highly localized.

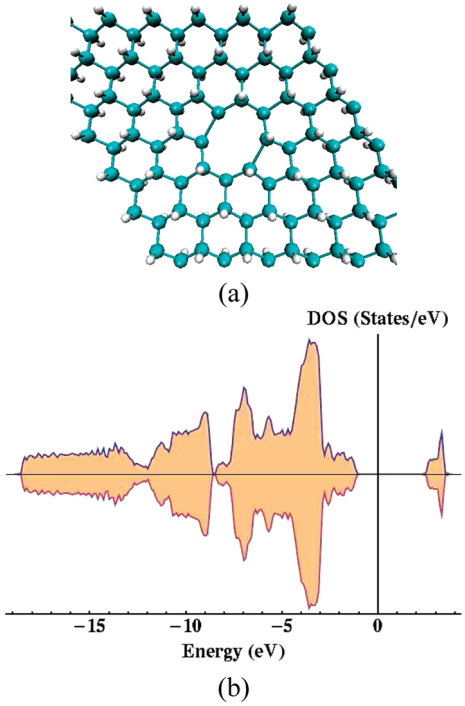

Figure 6. (a) Optimized structure of *graphane* with two vacancies for case 1 (see text). The rearrangement of the carbon atoms around the vacancies can be clearly seen. (b) Spin polarized DOS corresponding to the structure in part a. The DOS does not show any induced mid-gap states. Due to the rearrangement of the atoms, the band gap is reduced by 0.5 eV.

atoms. In fact the contribution from other carbon atoms turns out to be negligibly small. Interestingly, the hydrogen atoms associated with carbon atoms on the triangle do not show any

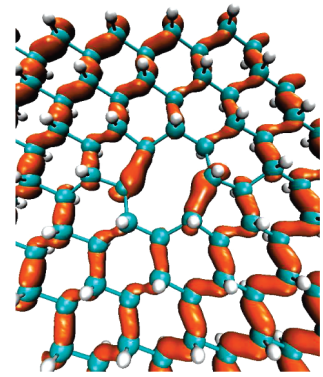

Figure 7. The charge density of the state at the top of the valence band. Two σ bonds formed by the rearrangement of carbon atoms are clearly seen.

TABLE 1: Energy Difference (Δ_E) with Respect to Lowest Energy System (i.e., Vacancies in Vicinity, $D = 1.52$ Å)[a]

	separation D			
	1.51 Å	2.52 Å	3.87 Å	10.71 Å
Δ_E (eV/atom)	0.0	0.0906	0.0185	0.0338

[a] D indicate the separation between the vacancies.

significant contribution. Furthermore the states turned out to be dominantly p_x-p_y-like.

Although there are states near the Fermi energy, these states need not necessarily conduct. Figure 5 shows the isosurface (at one-fifth of the maximum value) of the state just below the Fermi level. This state is induced due to removal of a carbon atom and is seen to be localized. A careful examination of the isosurfaces at the different values reveals that the induced state extends up to three to four nearest neighboring carbon sites. Thus the conduction mechanism through such orbitals may possibly be by hopping.

At this stage it is interesting to compare the nature of the induced state seen here to those seen in the case of graphene. As reported by several authors[9] the defects in the graphene structure also induce the states on the Fermi level. The contrast of such states with those in *graphane* is in the localization character. In the case of *graphane* the states are localized while in graphene those are known to be rather delocalized. The origin of such states is in the modification of the aromatic π-bonded delocalized states on a bipartitic lattice while in the case of *graphane* the states merely represent the unpaired electrons (dangling bonds).

3.3. Double Defect. The results of a single vacancy give enough impetus to study the effects of multiple vacancies, especially on the mid-gap states. Indeed, as we shall demonstrate, the nature and the placement of induced states is sensitive to the vacancy−vacancy interaction. This aspect brings in an interesting possibility of controlling the effective band gap via creation of vacancy defects.

For the purpose of this study we have used a larger supercell consisting of 192 atoms. Several possible scenarios emerge depending upon the separation of the two vacancies. We have examined four cases obtained by removing (1) the closest carbon pair (separation, $D = 1.51$ Å), (2) the nearest carbon atoms of the same sublattice ($D = 2.52$ Å), (3) a pair from different sublattice ($D = 3.87$ Å), and (4) two carbon atoms having large separation ($D = 10.71$ Å). In each of the cases we have fully relaxed the structure and have examined the energetics. We have found that the total energy is the lowest when the vacancies

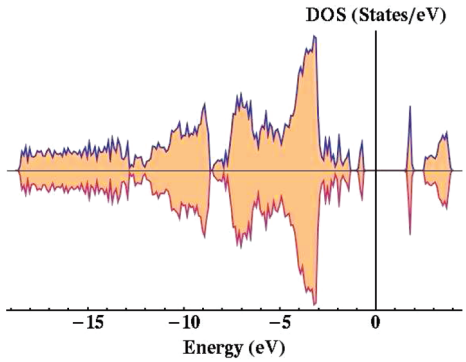

(a): 2.52 Å.

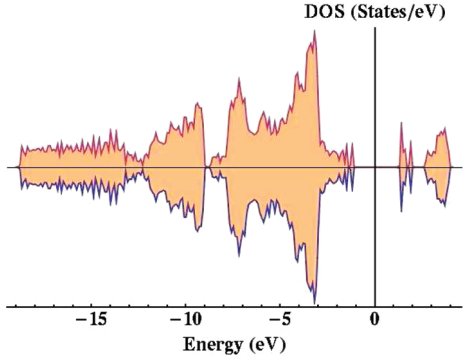

(b): 3.87 Å.

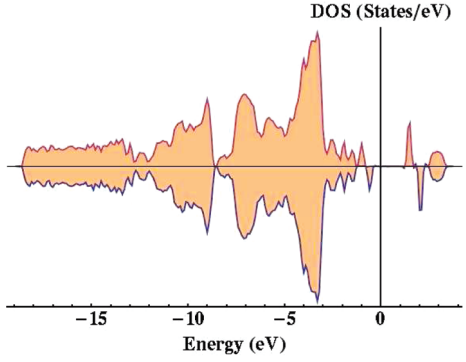

(c): 10.71 Å.

Figure 8. The DOS of *graphane* with two vacancies for cases 2, 3, and 4 (see text). For each of the cases the nature of the induced states is different. (a) The induced states appear near the conduction band for the vacancy separation of 2.52 Å. (b) For the vacancy separation of 3.87 Å the induced states are broadened, effectively reducing the gap from valence band. (c) A peculiar magnetic system with moment of 2 μ_B is seen for the vacancy separation of 10.71 Å. The induced states are near the conduction band and the states at the top of the valence band are substantially deformed.

are at the closest distance (case 1). The total energies with respect to the energy of the lowest energy system are shown in Table 1.

Figure 6 shows the optimized structure and DOS for case 1. Remarkably, the carbon atoms surrounding the vacancies rearrange to form two new σ bonds leading to the formation of a 5−8−5 ringed structure. This peculiar structure does not leave any unpaired electrons (dangling bonds) unlike the case of a single vacancy. This is consistent with the observation that there are no mid-gap states in the DOS as can be seen from Figure 6b. In this case the band gap is reduced by 0.5 eV with respect to pristine *graphane*.

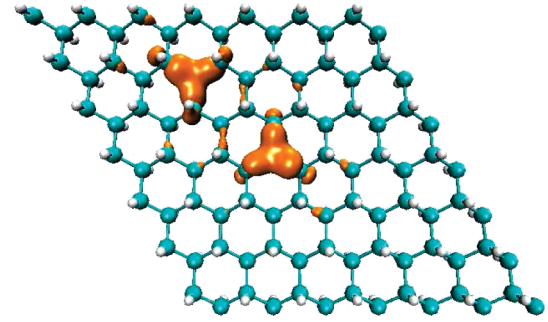

Figure 9. The charge density of one of the induced states of *graphane* with two vacancies separated from each other (case 2). The state is at the top of the valence band.

To ascertain the formation of σ bonds we have examined the charge densities of some relevant states. Figure 7 shows the charge density of a state at the top of the valence band (occupied state). The charge clearly depicts the formation of σ bonds among the carbon atoms. We have also seen that the bands at the bottom of the conduction band (figure not shown) are highly delocalized with almost no charge around the vacancy site.

A different scenario emerges when the vacancies are separated from each other. Now there are induced states in the gap. Figure 8 shows the DOS for the three cases with the vacancy separation of (a) 2.52, (b) 3.87, and (c) 10.71 Å. Quite clearly in the case of well-separated vacancies, the atoms are not able to rearrange so as to form any bonds. This leaves six unpaired electrons. These unpaired electrons give rise to the mid-gap states, typically just above the valence band and just below the conduction band. Interestingly their placement is sensitive to the separation between the vacancies. For example, Figure 8a shows the DOS for the vacancy separation $D = 2.52$ Å. The induced states are seen at about 0.5 eV below the conduction band along with the additional modifications at the edge of the valence band. As the separation increases to 3.87 Å (Figure 8b) the induced states are broadened with a width of about 1 eV and split into two distinct peaks. In most of the cases the unpaired electrons tend to cancel the spin giving rise to nonmagnetic states. However, for a large separation, i.e., in the limit of weakly interacting vacancies, both vacancies carry a magnetic moment of 1 μ_B. Figure 8c shows the DOS for the system with a vacancy separation 10.71 Å, depicting on the spin polarized features.

The induced states are seen to be localized, both in the case of single as well as double vacancies. Figure 9 depicts the charge density isosurfaces of a typical state for case 2 ($D = 3.87$ Å). The state is at the top of the valence band and is completely occupied. The isosurface is plotted at a lower value (one tenth of the maximum). Clearly the state is dominantly p-like and is localized. Even at such a lower value of isosurface we see a weak overlap on the carbon atoms. Naturally for the higher value of the isosurface the lobes are disconnected.

Apart from the four cases discussed above, we have also calculated the electronic structure and DOS for a few more vacancy separations. The results indicate that the sublattice plays no role in appearance on mid-gap states. This is a remarkable contrast to the case of graphene where almost all the properties are dependent on its sublattice.

4. Conclusions

We have carried out an ab initio investigation on the electronic structure of *graphane* with single and double vacancy defects. For both cases, we have analyzed the fully optimized structure, and have examined the DOS and charge densities as a function of separation of the vacancies. Our calculations show that the most stable structure is obtained when the vacancies are adjacent to each other, accompanied by the reduction of band gap. In this case there are no induced mid-gap states. However, separated vacancies induce mid-gap states and interestingly their position and width are sensitive to the vacancy separation. Although the separation between the vacancies plays a crucial role we do not find a significant role for the sublattice in the appearance of the states. Examination of the charge densities of the induced states shows that these states are localized. Our calculation brings out the possibility of manipulating the band gap and the nature of the mid-gap states with the aid of vacancy defects in *graphane*.

Acknowledgment. B.S.P. would like to acknowledge CSIR, Government of India for financial support (No. 9/137(0458)/2008-EMR-I). It is a pleasure to acknowledge the Center for Development of Advanced Computing for computational resources. Some of the figures are generated by using VMD software.[15]

References and Notes

(1) Sofo, J. O.; Chaudhari, A. S.; Barber, G. D. *Phys. Rev. B* **2007**, *75*, 153401.

(2) Boukhvalov, D. W.; Katsnelson, M. I.; Lichtenstein, A. I. *Phys. Rev. B* **2008**, *77*, 035427.

(3) Casolo, S.; Løvvik, O. M.; Martinazzo, R.; Tantardini, G. F. *J. Chem. Phys.* **2009**, *130*, 054704.

(4) Elias, D. C.; Nair, R. R.; Mohiuddin, T. M. G.; Morozov, S. V.; Blake, P.; Halsall, M. P.; Ferrari, A. C.; Boukhvalov, D. W.; Katsnelson, M. I.; Geim, A. K.; Novoselov, K. S. *Science* **2009**, *323*, 610–613.

(5) Fuhrer, M. S.; Adam, S. *Nature* **2009**, *458*, 38–39.

(6) Pereira, V. M.; dos Santos, J. M. B. L.; Neto, A. H. C. *Phys. Rev. B* **2008**, *77*, 115109.

(7) Pereira, V. M.; Guinea, F.; dos Santos, J. M. B. L.; Peres, N. M. R.; Neto, A. H. C. *Phys. Rev. Lett.* **2006**, *96*, 036801.

(8) Yazyev, O. V.; Helm, L. *Phys. Rev. B* **2007**, *75*, 125408.

(9) Neto, A. H. C.; Guinea, F.; Peres, N. M. R.; Novoselov, K. S.; Geim, A. K. *Rev. Mod. Phys* **2009**, *81*, 109.

(10) Jin, C.; Lan, H.; Peng, L.; Suenaga, K.; Iijima, S. *Phys. Rev. Lett.* **2009**, *102*, 205501.

(11) Lebègue, S.; Klintenberg, M.; Eriksson, O.; Katsnelson, M. I. *Phys. Rev. B* **2009**, *79*, 245117.

(12) Kresse, G.; Furthmüller, J. *Phys. Rev. B* **1996**, *54*, 11169.

(13) Perdew, J. P.; Burke, K.; Ernzerhof, M. *Phys. Rev. Lett.* **1996**, *77*, 3865.

(14) Perdew, J. P.; Burke, K.; Ernzerhof, M. *Phys. Rev. Lett.* **1997**, *78*, 1396.

(15) Humphrey, W.; Dalke, A.; Schulten, K. *J. Mol. Graphics* **1996**, *14*, 33–38.

JP907640T